

# Reversible On–Off of Chirality and Anisotropy in Patterned Coexistence of Achiral-Anisotropic and Chiral-Isotropic Soft Materials

Qinyu Mo, Binghui Liu, Wenbin Huang, Pei-Zhi Sun, Zhiying Li, Hari Krishna Bisoyi, Dong Shen, Zhi-Gang Zheng,\* Yan-Qing Lu,\* and Quan Li\*

Achieving a coexistence of two or multiple phases of soft matters via a delicate trade-off of free energy and long-range order with one another has been inspiring abundant interest on fundamental sciences and engineering. In this work, a stable coexistence of the optically achiral-anisotropic liquid crystalline nematic phase and the optically chiral-isotropic liquid crystalline blue phase is proposed and demonstrated, with their distribution tailored in a micro-pattern by the developed localized micro-regional polymer templating technique. Such a stable patterned coexistence of the two different phases with a distinct molecular arrangement, optical chirality, and anisotropy is achieved depending on a delicate matching of the elastic energy on the interface between liquid crystals and polymer networks. In contrast to the majority of soft coexistence systems, a specific dynamic and reversible on–off response of chirality and anisotropy is observed in such a system driven by an electric field. The structure of patterned coexistence system in the presence and absence of external stimulation is explored by microscopy and optical technique, and furthermore, the prospective photonic applications are demonstrated. This investigation indicates another category of functional soft material with fantastic adaptive characteristics for application in optics, electronics, interface physics, and chemistry.


Soft coexistence system, composed of two or more categories of soft condensed matters with distinct molecular arrangement and symmetry, self-organization behavior, long-range order, and phase transition dynamics from one another, is opening pathways for flexibly engineering of multifunctional soft materials that exhibit improved or fantastic characteristics toward implementation in emerging domains like wearable electronics,<sup>[1,2]</sup>

soft robotics,<sup>[3,4]</sup> biohybrid engineering,<sup>[5]</sup> etc. Such a soft coexistence is commonly adopted in polymer engineering to essentially improve characteristics of specific aspects or achieve novel properties such as good biological compatibility, excellent mechanical strength, and high chemical resistance through intramolecular interactions via covalent bonding or intermolecular van der Waals force via polymer chain stacking conformations. Contemporarily, there are two categories of polymer coexistence systems: one is the heterogeneous polymer coexistence system made up of compatible polymer constituents,<sup>[4,6]</sup> and the other is the multiple phase polymer coexistence system<sup>[7]</sup> consisting of two or more incompatible polymer constituents, which is more prevalent.<sup>[8–11]</sup> The distributed domains of different phases in multiple phase polymer coexistence systems vary from several nanometers to tens of micrometers and interact with each other for spurring extraordinary physico-chemical properties, which has attracted much attention.<sup>[12–14]</sup>

Liquid crystals (LCs) are emerging as intelligent soft material systems with appealing supramolecular self-organization and stimuli-responsive capabilities for novel optical, energy, and electronic applications.<sup>[15–18]</sup> The phase behaviors and thus the unique functionalities of LCs depend on their self-organized architectures, such as the achiral nematic (N) phase with orientational ordering having a prominent optical anisotropy;

Q. Mo, B. Liu, Prof. W. Huang, P.-Z. Sun, Z. Li, Prof. D. Shen, Prof. Z.-G. Zheng  
Department of Physics  
East China University of Science and Technology  
Shanghai 200237, China  
E-mail: zgzheng@ecust.edu.cn

Prof. W. Huang  
School of Optoelectronic Science and Engineering & Collaborative  
Innovation Center of Suzhou Nano Science and Technology  
Soochow University  
Suzhou 215006, China

 The ORCID identification number(s) for the author(s) of this article can be found under <https://doi.org/10.1002/adom.202000155>.

Dr. H. K. Bisoyi, Prof. Q. Li  
Advanced Materials and Liquid Crystal Institute and Chemical Physics  
Interdisciplinary Program  
Kent State University  
Kent, OH 44242, USA  
E-mail: qli1@kent.edu

Prof. Y.-Q. Lu  
National Laboratory of Solid State Microstructures  
Collaborative Innovation Center of Advanced Microstructures  
and Colleague of Engineering and Applied Sciences  
Nanjing University  
Nanjing 210093, China  
E-mail: yqlu@nju.edu.cn

DOI: 10.1002/adom.202000155

the cholesteric phase, containing the periodic helical superstructure, with a specific optically chirality; and another chiral phase, blue phase (BP), having a fantastic cubic superstructure stacked by double twisted LC cylinders, that is, the simple cubic BPII and the body-centered cubic BPI, showing optical isotropy. The miscibility kinetics, phase transition thermodynamics, and the relevant characteristics for the coexistence system of such a fluid soft matter and common liquids have become thriving topics to explore their potential as a novel platform of soft materials, which enriches abundant and unpredictable physical behaviors and fantastic optical and flow properties of both scientific and technological interests, due to the interplay of the interface elastic forces at the domain contour and the optical coupling arising from the anisotropic LC and isotropic liquids. For instance, numerical calculations indicate that the coexistence system of the optically chiral and isotropic blue phase liquid crystal (BPLC) and the common optically achiral and isotropic liquid exhibits specific physical and morphology behaviors deriving from the contest between interfacial and elastic energies at different length scales.<sup>[19]</sup> Experimentally, small droplets of BPLC in deionized water show significantly different phase behaviors as compared with their bulk counterpart and the defect structure, reflection color, and morphology can be manipulated by adjusting the interfacial parameters such as the droplet size and anchoring conditions.<sup>[20,21]</sup> In addition, tunable and omnidirectional micro-cavity for generating a fantastic laser emission was obtained by dispersing the cholesteric LC in glycerol as microdroplets.<sup>[22]</sup>

In this regard, the soft coexistence system of different LC phases such as the optically achiral-anisotropic N phase and the optically chiral-isotropic BP could imply numerous mutual concerned fundamental issues and potential applications, as the cubic superstructure of BP with a lattice constant of a few hundred nanometers and the N phase contains uniformly aligned LC molecules, which are expected to be combined together to open the possibility for designing and establishing a desirable soft coexistence system capable of exhibiting promising properties and device applications. Such a coexistence system could show synergistic characteristics not shown by any individual LC phase itself and provide sufficient insights into the interaction dynamics among these dispersed phase regions, stimulated by the complex coupling effects caused by the fluctuation of orientation field at different phase domain boundaries. However, the realization of such a stable coexistence is a formidable task limited by the current fabrication techniques and materials. First, the stabilization of BP, especially the simple cubic BPII, is a sophisticated chemical–physical process dominated by the interplay among various factors, which requires a delicate balance between the intermolecular interaction and the topological constraint, resulting in a frustrated system with a common temperature range normally less than several Kelvins. Structural stabilization of BP<sup>[23–27]</sup> via polymer network has been implemented to extend the BP temperature range to purposefully ensure practical applications such as displays,<sup>[24]</sup> organic lasers,<sup>[25]</sup> and tunable filters.<sup>[26]</sup> However, the achievement of a stabilized BP in a soft coexistence system with other LC phases is still challenging. Adopting a specific stimuli-activated material to selectively unwind helical arrangement of LC might be a possible approach to obtain a phase coexistence,

whereas the instability is still an inevitable problem. Second, the complex and fragile cubic superstructure formed by double twisted LC cylinders in the BP is susceptible to the NLC alignment at the phase boundary through the long-range cooperative molecular interaction, making the coexistence of the chiral-isotropic cubic superstructures with achiral-anisotropic nematic domains extremely difficult in typical LC material systems.

In this work, a soft patterned coexistence system, having a satisfying thermal stability, consisting of the optically chiral-isotropic liquid crystalline BP and the achiral-anisotropic N phase with dynamic and reversible responsive chirality and anisotropy has been established as prescribed through an ingenious micro-regional patterned polymer templating technique. Such a bi-phase coexistence presents the prominent coupled optical characteristics, which are essentially distinct with those of the individual phases, and holds the possibility of arbitrarily tailoring the pattern of coexistence system by selectively distributing the micro-regions of BP and N phase as the predesigned pattern. It is worth noting here that such a patterned coexistence system has a specific dynamic and reversible responsive chirality and anisotropy property driven by an appropriate electric field and exhibits a reversible transformation among the original optically achiral-anisotropic and chiral-isotropic coexistent system (i.e., consisting of N phase and BP), achiral/chiral but entirely isotropic system caused by the homeotropic alignment of nematic constituent stimulated by a lower electric field, and the uniform achiral and isotropic system resulted from the strong field-induced unwinding of chiral BP, provoking a striking stimuli-responsive behavior which is capable to extend the common understanding of soft material. This work not only provides a facile approach to obtain the stable soft patterned coexistence system but also sheds light on the fascinating properties of this optically achiral-anisotropic and optically chiral-isotropic soft liquid crystalline coexistence with both scientific significance and technological potentials.

The soft liquid crystalline coexistence system composed of the optically achiral-anisotropic N phase and optically chiral-isotropic BP, distributing as an alternate and programmable micro-pattern, was achieved by the localized micro-regional polymer templating technique, in which the localized polymer networks preserve the molecular organization information and induce a BPII arrangement and restrain the distribution of BPII and N phase in a versatile and effective way. The initial chiral LC mixture, generating a BPII arrangement via a delicate manipulation of the ambient temperature from 34 to 36 °C (Figure S1, Supporting Information) was composed of nematic LCs (NLCs), 3.5 wt% chiral dopant, and 15 wt% reactive acrylate-based monomers. A small amount of photoinitiator was also added to the mixture to initiate the polymerization of reactive monomers. The mixture was then cured in a cell in its BPII state by a prescribed patterned light illumination through a corresponding photo-mask, resulting in a stable BPII arrangement of LC molecules over a broad temperature range bounded by the densely crossed-linked polymer networks in exposed regions. Afterward, the entire sample was preserved to the room temperature; it is noteworthy that in the unexposed regions the unstable BPII transformed to a cholesteric phase due to the phase transition (Figure 1). The light exposed cell was then immersed in dichloromethane to wash the host LC

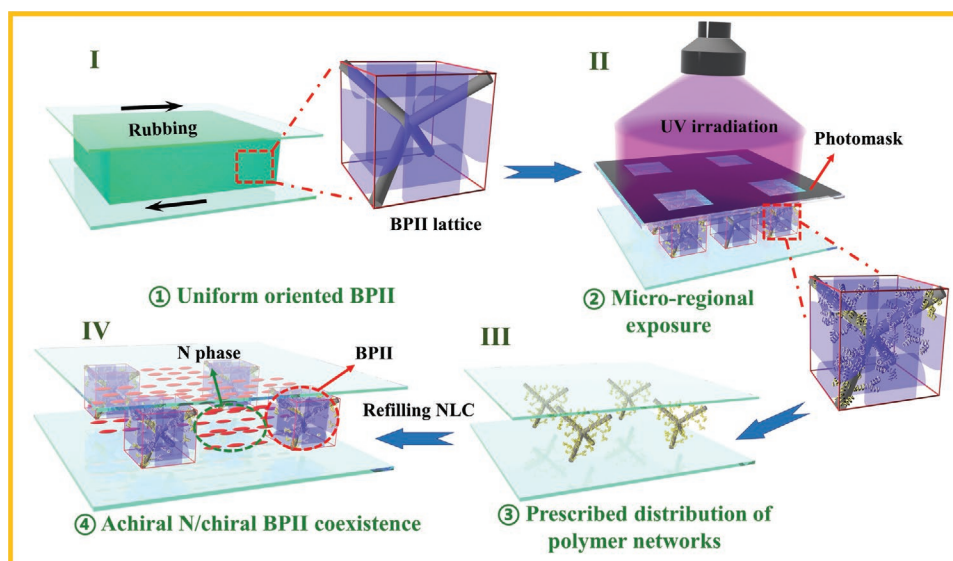


**Figure 1.** Patterned soft coexistence of the optically achiral-anisotropic N phase and optically chiral-isotropic BPII achieved by the localized micro-regional polymer templating technique. Illustration of the soft matter coexistence system fabrication process which consists of steps of cooling from the isotropic phase to the BPII (I), patterned photo-polymerization (II), removal of the chiral LCs (III), and refilling of the achiral LC (IV) (see Experimental Section for more details). The delicate polymer networks preserve the information concerning the chiral LC alignment and transfer it locally to achiral LC via molecular interactions.

and unreacted monomers and oligomers, leaving the square-patterned polymer micro-regions of  $60 \times 60 \mu\text{m}^2$  dimensions periodically distributed on the substrate with a space of  $120 \mu\text{m}$  between the adjacent squares (Figure 1-III). Such a dense polymer network of every square template provided a strong interfacial elastic interaction on LCs, thereby ensuring an effective reconfiguration of a stable BP arrangement by refilling either the cholesteric LCs with a handedness same or opposite to the BP or even the achiral NLCs host (Figure S2, Supporting Information), and therefore facilitating the design and establishment of a patterned bi-phase coexistence system.

Subsequently, we targeted to configure an ingenious coexistence of the chiral-isotropic BP and the achiral-anisotropic N phase via refilling common achiral NLCs into such a patterned polymer template (Figure 1-IV). Once LCs infiltrated into the polymer regions, that is, exposed areas, the original arrangement and long-range order of them were forced to form a simple cubic BP arrangement reserved in the polymer networks, displaying the square-shaped bluish microscopic texture with a sharp boundary and similar transverse dimension as the polymer regions (Figure 2a-II). It should be noted that the alignment of LCs out of the polymer regions, that is, the unexposed areas, was unidirectional as determined by the surface anchoring of the cell substrates, thus ensuring a coexistence of two different liquid crystalline phases, with the BP regions confined in periodically distributed squares embedded into the homogeneously aligned N phase (Figure 2a-II), which were similar to the original BP before washing the LCs out of the polymer network (Figure 2a-I). Commonly, the simple cubic BPII is less stable than the body-centered cubic BPI due to the lower lattice packing ratio for the former; thus, achieving a more stable BPII is still a challengeable topic. Herein, BPII was stabilized cautiously to indicate the robustness of the proposed approach in obtaining different soft coexistence systems. The

reflection spectral line shape of the reconfigured BP, including the bandwidth and the reflection intensity, was almost invariable, although the entire spectrum showed a slight blue-shift compared to the original BP, which could be due to the shrinkage of the polymer network after washing. Such a selective reflection of BP was dependent on the handedness of an impinged circular polarized light (Figure S3, Supporting Information), that is, only the light having the same handedness with the BP can be reflected, therefore confirming the optical chirality of BP regions. The scanning electron microscope (SEM) micrograph showed the regular array of polymer squares adhered onto the bare substrate (Figure 2a-III). The thickness of the polymer film is around  $1.6 \mu\text{m}$ , which was thinner than the cell gap ( $4 \mu\text{m}$ ). The shrinkage of the film after solvent evaporation was attributed to the de-swelling effect. Since the LC was removed by the solvent, holes were left in the polymer film initially occupied by LCs, which would collapse as the solvent evaporates.<sup>[28]</sup> No polymer fiber was observed between the neighboring polymer squares, thereby confirming the interfacial effect between polymer and LCs on the construction of such an achiral/chiral bi-phase coexistence. The distinguishable lamellas tightly stacked layer-by-layer were presented at the cross profile of the polymer region as shown in the inset, which was a typical characteristic of the BP system. The Kössel diagram, presenting an almost unchanged circular ring between the original and reconfigured simple cubic BP (Figure 2b-I,III), caused by the lattice diffraction and depended on the crystallographic orientation, was detected in the case of a monochromatic light irradiation of 450-nm laser, which further manifested the architecture of BPII induced at polymer regions. The unidirectional alignment behavior of NLC molecules at the unexposed regions was attributed to the strong anchoring of the polyimide (PI) alignment layer on the surface of the cell. To further explore such interfacial effect, the contact angle of



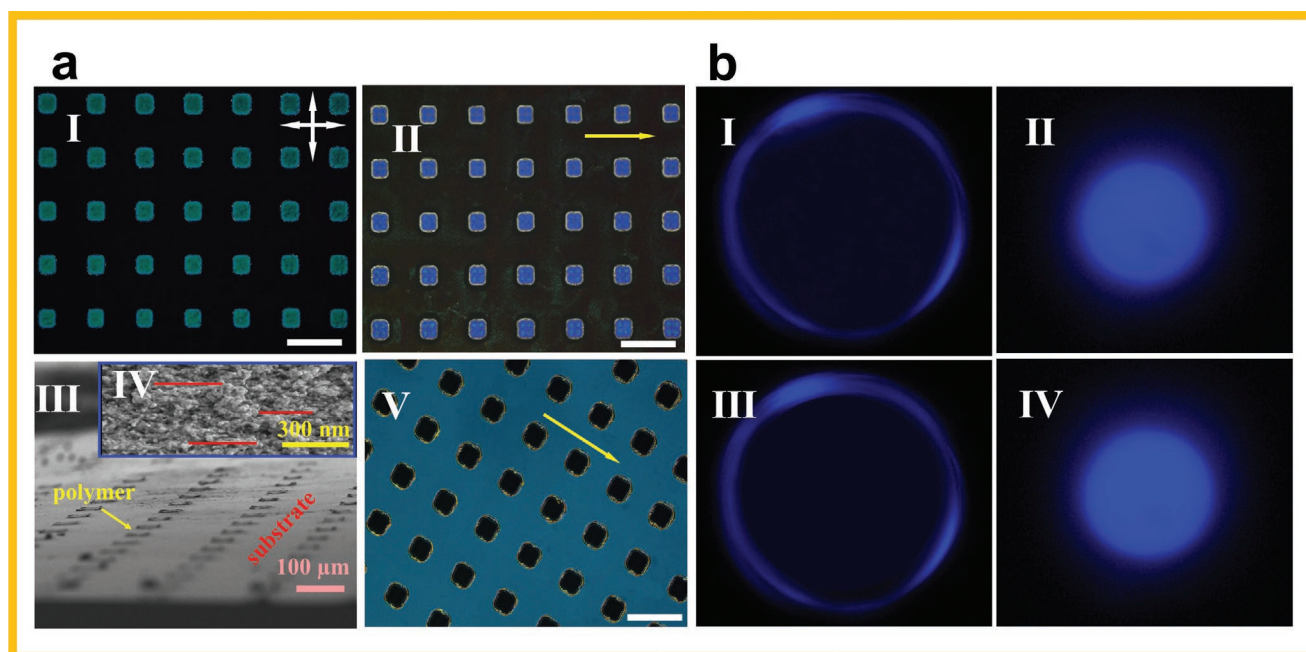


**Figure 2.** The POM images and Kössel diagrams of the bi-phase coexistence. a) Room-temperature microscopy images of the bi-phase coexistence system in the unidirectionally anchored cell. The reflection POM image of the initial chiral/chiral LC mixture (I) and the bi-phase coexistence of achiral-anisotropic N phase and chiral-isotropic BP (II) with a parallel orientation. The SEM image of the polymer film at a monomer concentration of 15 wt% after washing out the LCs; surface morphology (III), the scale bar (pink line) is 100  $\mu\text{m}$ ; sectional morphology (IV), the scale bar (yellow line) is 300 nm. The transmission POM image of the achiral-anisotropic and chiral-isotropic coexistence with 45° orientation (V). The microscope polarizers are crossed and the yellow arrow denotes the nematic director orientation. The scale bar (white line) is 200  $\mu\text{m}$  (I, II, and V). b) Room temperature micro-regional Kössel diagrams in the initial chiral/chiral bi-phase LC mixture, from the BP regions (I) and the CLC regions (II); and in the coexistence of achiral-anisotropic N phase and chiral-isotropic BP, from the BP regions (III) and the N phase regions (IV).

NLCs on the surface of the alignment film and polymer network were detected, respectively, which showed a contact angle of 18.5° for the former (Figure S5a-I, Supporting Information) and 32.5° for the latter (Figure S5b-I, Supporting Information), thus confirming the weaker surface tension of NLCs on polymer network compared with that on PI, which indicated that the alignment behavior of NLCs at the unexposed regions was dominated by the anchoring provided by PI film. Such alignment behavior of NLCs was further evaluated from the optical texture under the transmission mode polarizing optical microscope (POM), which displayed a cyan-colored bright state (Figure 2a-V) when rotating the sample resulted from the birefringence of the unidirectional aligned LCs, thus indicating the optical anisotropy of the homogeneously aligned NLCs. On the contrary, BP regions showed an invariable dark state due to its optical isotropic characteristics. No typical Kössel diagram was observed at the unexposed regions as predicted for the reason that the lattice symmetry was absent in such a cholesteric phase and an achiral N phase (Figure 2b-II,IV).

Such a stable bi-phase existence was probably caused by a delicate trade-off of the chiral interaction and the interfacial effect. Our experiments indicated an interesting dependence on the concentration of the acrylate-based monomers and was elaborately optimized as 15 wt% (Figure S4, Supporting Information). When the monomer concentration was below such an optimization, the polymer network was either too loose to reconfigure BP superstructure, or insufficiently robust to stabilize a reconfigured BP. On the other hand, a higher monomer content,

for instance 17 wt%, played a negative role on the construction of the bi-phase coexistence, caused by severe migration and polymerization of molecules during the light irradiation which promoted a random and undefined phase separation between polymer and LCs and thereby blurred the boundary between achiral N phase and chiral BP.

The distributions of reflection intensity and birefringence of the bi-phase coexistence indicate that the regularly periodic high intensity regions, corresponded to BP, prominently stood out on a low intensity N phase background in the case that the director of N phase was parallel or orthogonal to the transmission axis of one of the polarizers fixed on POM (Figure 3a-I). The rotation of the sample for about 45° significantly enhanced the reflection intensity at the region of N phase due to the interference of ordinary and extraordinary components in the case of a unidirectional alignment at N phase region (Figure 3a-II); however, reflection intensity at BP region still remained invariable, which further confirmed its optical isotropy. Birefringence distribution of the entire sample is an efficient aspect of corroborating the structure of such a bi-phase liquid crystalline coexistence arising from the distinctly different optical property between N phase and BP, that is, optical anisotropy for the former and isotropy for the latter. A monochromatic 633-nm laser was used as a probe beam to detect the birefringence of N phase and BP regions based on the conventional Senarmont's compensation method. The legible BP squares, labeled as dark bluish colour, meant a relatively lower birefringence of less than 0.01, regularly embedded in the bright yellowish nematic

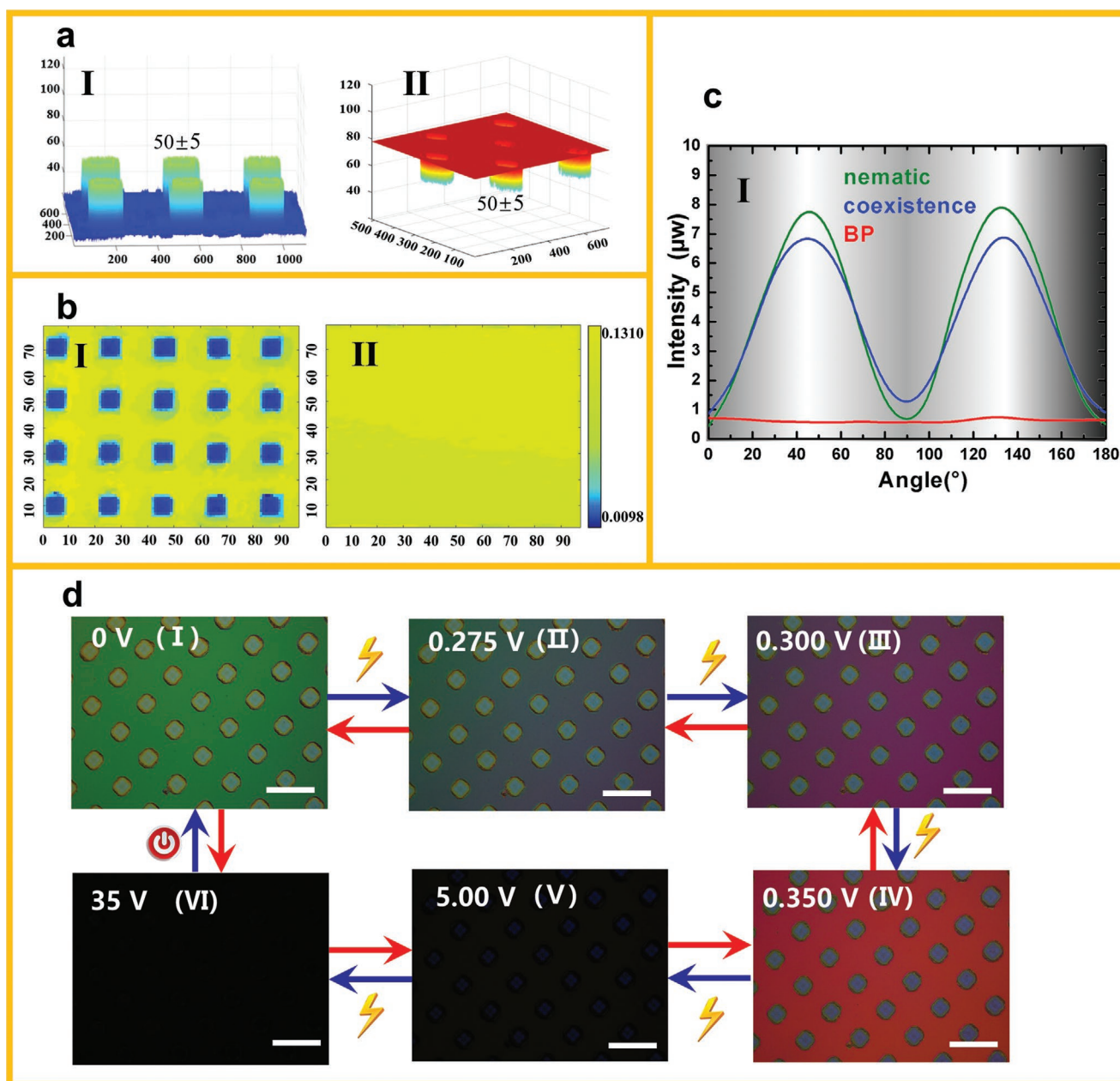


**Figure 3.** Reflection intensity, birefringence performance, and its electric tunability of the bi-phase coexistence of achiral-anisotropic N phase and chiral-isotropic BP. a) Intensity distribution of the reflection POM image for bi-phase coexistence with the orientation of the N phase to the receiver polarizer being 0° (I) and 45° (II). b) Birefringence distribution of the bi-phase coexistence (I) and the pure N phase (II). c) The dependence of the transmission intensity on the angle between the sample orientation and polarizer (perpendicular to the analyzer) for the pure BP (the red line), the pure nematic phase (the green line), and the N/BP bi-phase coexistence (the blue line). d) Reflection POM images of the bi-phase coexistence at different applied voltages. The scale bar is 200 μm.

background (Figure 3b-I) denoting a comparable higher birefringence of about 0.13 which was a sufficient consistency with the value in the case of a homogeneous alignment under the same condition (Figure 3b-II), thus manifesting an almost negligible influence of the polymer interface on the alignment behavior of N phase regions. The bi-phase coexistence technique to strategically “knead” one optically anisotropic phase together with another optically isotropic one might be an efficient approach to conveniently modulate the birefringence of

the LCs confined in such a thin cell by varying the shape, size, or the density of the BP area through a prescribed patterned exposure without the aid of any external stimuli, such as electric field and light. Thus, the very tedious and trivial mixing according to a delicate formulation, which is always adopted in LC industry, can be bypassed. To corroborate the variation of birefringence when inserting the BP into the N phase, the samples were placed between a pair of crossed polarizers to test the dependence of transmission intensity on the angle of

alignment direction relative to the transmission axis of one polarizer. Figure 2c demonstrates the alternate modulation with a similar period, that is, bright state at the angle of  $45^\circ$  while dark state at  $90^\circ$ , but lower bright/dark contrast for the coexistence system compared with the sample NLCs. However, the BPLC showed just a faint modulation which further corroborates its attribute of optical isotropy. Birefringence of the NLC and the coexistence system were calculated via the aforementioned dependencies as 0.130 for the former and 0.109 for the latter, thus quantitatively confirming a validity of birefringence modulation by embedding such an optically isotropic phase into the anisotropic medium.

One attractive characteristic of the bi-phase coexistence system is a unique dynamic and reversible responsive optical chirality and anisotropy driven by an external electric field, which has not been observed or demonstrated so far. As shown in Figure 3d, a brilliant color evolution at the nematic regions, which changed from the original green, passing through a bluish purple, to a bright red (Figure 3d-I–IV) was found with the enhancement of the applied voltage (i.e., electric field) due to the electric field controlled birefringence of LCs via field-induced Fréedericksz transition. It was interesting that the arrangement of BP regions was almost invariable under the stimulation of such a weak electric field resulting from the strong restraint of polymer network on molecular rotation of LCs. As the voltage was enhanced to 5 V (Figure 3d-V), the BP arrangement was still maintained but the homogeneously aligned N phase transitioned to homeotropic alignment (i.e., aligned along the cell normal) with optical isotropy, thus stimulating the coexistence from the original coexistence of achiral (N)/chiral (BP) and anisotropic (N)/isotropic (BP) to the achiral (N)/chiral (BP) but entirely isotropic one (Figure S6, Supporting Information). Further increasing the voltage to the saturation of 35 V (Figure 3d-VI) led to the unwinding of chiral BP, thus transformed the entire sample to achiral and isotropic homeotropic alignment. The entire process was also corroborated by a real-time reflection spectrum evolution of the sample, which showed an asynchronous attenuation of the BP reflection band and the broadband corresponding to the nematic region (Figure S7, Supporting Information). Such a unique soft bi-phase coexistence, which can be reversibly manipulated from the initial achiral/chiral and anisotropic/isotropic state to the achiral/chiral but entirely optically isotropic state with a weak electric field and even can be transformed to a uniform achiral and isotropic homeotropic state by a strong unwinding electric-field, has not been accomplished previously. Such unique system may provide some innovative insights and specific perspectives to investigate the self-organization, structural construction, and interfacial interaction of the soft matters.

The distribution of BP and N phase in such patterned coexistence system, either the shape or the size, can be tailored via a judiciously predesigned patterned polymer template formed in the process of patterned exposure of prepolymerized mixture with the optimized conditions, so as to re-establish an equilibrium between the achiral–chiral interaction and interfacial free energy of the system. Figure 4a-I shows an inverse patterned coexistence relative to the aforementioned one (Figure 2a-II), that is, the square regions were occupied by N phase while the other areas were BP. Changing the exposure pattern to stripes

can reconfigure a coexistence with the corresponding periodic stripe-pattern (Figure 4a-II). The regular patterned distribution of BP and N phase, and the sharp BP/N interface manifested that the delicate equilibrium between achiral–chiral interaction and interfacial free energy efficiently disturbed the long-range orderliness near the interface in a variety of patterned BP/N coexistences. The corresponding diffraction patterns detected in the case of a normal impinging of the He-Ne laser exhibited a conspicuous missing of the  $\pm 3$ rd order (Figure 4a-III,VI) resulting from the refractive index modulation of two different phases with an almost square wave profile (a duty ratio of 1:2), which further corroborated the well-defined patterned coexistence and a sharp boundary of the refractive indices of the two regions of the BP phase and N phase.<sup>[29]</sup> Moreover, such diffraction presented a prominent polarization dependency due to the optical anisotropic N phase in the system. The first-order diffraction efficiency of the inverse patterned coexistence sample (i.e., Figure 4a-I) was tested at different phase modulations by changing the angle between the polarization direction of a linear probe beam and the orientation of N phase, which showed good agreement with the calculation based on scalar diffraction theory (Figure 4a-VII). Such agreement also indicated a satisfying regularity, either in shape or size, of phase distribution in the bi-phase coexistence system. Furthermore, a very fantastic multi-mode display which can be switched without any external fields, such as electric field, light, temperature, and mechanic force, was demonstrated by designing the heart-shape and English alphabets “LC” BP regions in a background of N phase (Figure 4b-I,II). It can be predicted reasonably that the bi-phase coexistence system located between two crossed polarizers has three stable display modes: 1) a reflection-mode displaying the colored exposed pattern (BP), such as the periodic stripe-pattern (Figure 4a-II); 2) a transmission-mode with the nematic director parallel or perpendicular to incident light polarization, displaying the erasing of the exposed pattern (i.e., BP region) (Figure 4a-IV); 3) a transmission-mode but with a slanted angle between the nematic director and the incident light polarization, displaying the bright unexposed pattern (i.e., N region) with controllable intensity and birefringent color (Figure 4a-V). Such display modes can be switched by changing either the viewing direction or the angle between the nematic director and the analyzer through a rotation of the sample without any additional external fields. The tri-state passive display has some specific advantages, such as low energy consumption and high stability, and is expected to be applied to static display devices such as indoor and outdoor publicity, advertising, and labels.

Microcavity lasers are emerging as the compact light sources for photonic integrated circuits, lab-on-chip sensing, and quantum single photon lighting due to their excellent spectral monochromaticity, emission directionality, and on-chip integrity.<sup>[27]</sup> To date, there are micro-resonator configurations at different sizes to efficiently stimulate laser emission such as the micrometer-scale spheres and rings,<sup>[30]</sup> the subwavelength photonic-crystals,<sup>[31]</sup> and the super diffraction limit plasmonic cavities.<sup>[32]</sup> It was noted that such bi-phase coexistence system had two periodic structures for light confinement and resonance: one was the micrometer-scale distribution of BP and N phase regions and the other was the subwavelength-scale BP lattice, and the light coupling between the two resonations



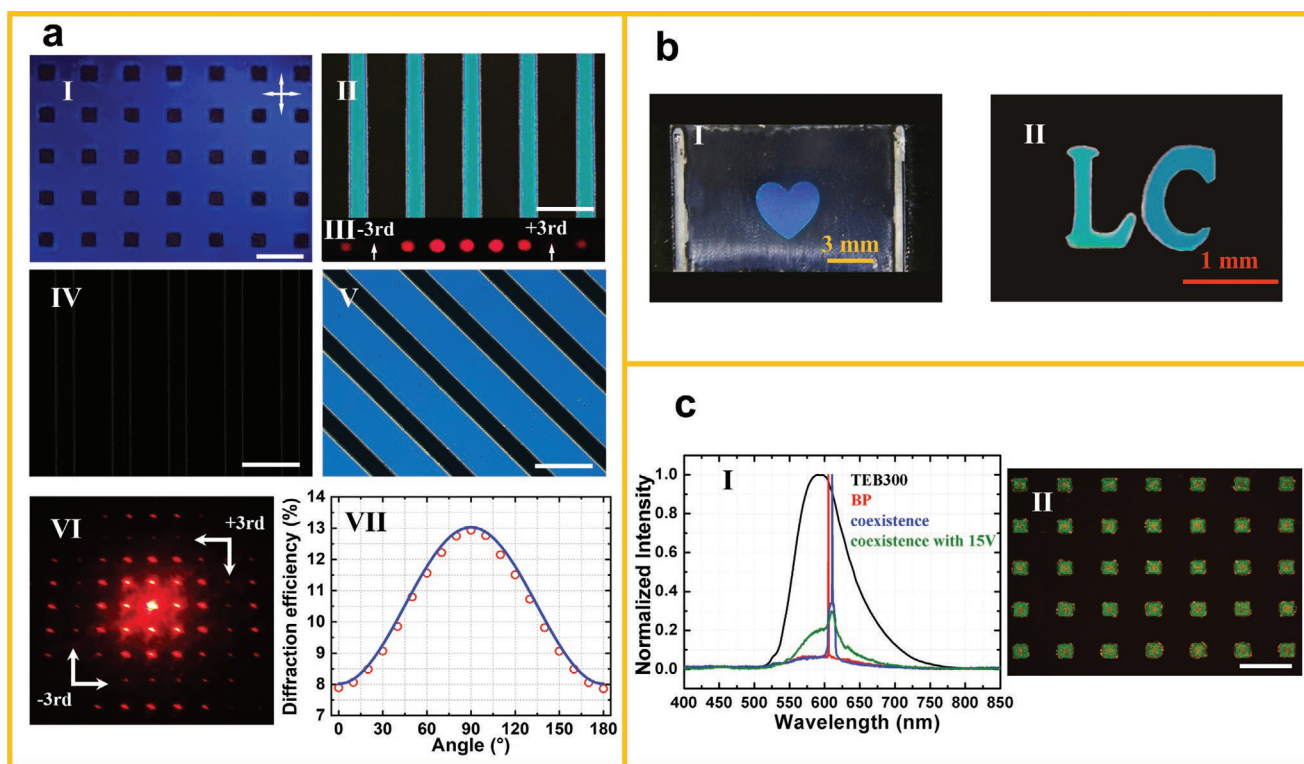


**Figure 4.** The dynamic N/BPII bi-phase coexistence as a new platform for photonic applications. a) Different N/BPII coexistences for diffraction and displaying applications. Reflection POM image of the N/BP coexistence containing 2D complementary squares (I) and periodic stripes (II). The scale bar (white line) is 200  $\mu\text{m}$ . The corresponding diffraction patterns under the illumination of a linearly polarized He-Ne laser indicates the absence of the  $\pm 3\text{rd}$  order diffractions (III, VI). The transmission POM image of the N/BP coexistence with periodic stripe-pattern with the orientation of the N phase to the receiver polarizer being  $0^\circ$  (IV) and  $45^\circ$  (V). The first-order diffraction efficiency of the complementary square N/BP coexistence sample was tested with the different angles between the polarization direction of a linear probe beam and the orientation of N phase. The blue curve is the theoretical value and the red circle is experimental value (VII). b) Reflection POM image of the bi-phase coexistence with a patterned BP phase into the heart shape (I), the scale bar (yellow line) is 3 mm; and English alphabets “LC” (II) under crossed polarizers, the scale bar (red line) is 1 mm. c) The bi-phase coexistence as a novel micro-resonator for organic lasing. The laser spectra of the pure nematic phase (the black line), the pure BP (the red line), the N/BP coexistence without voltage (the blue line), and with the voltage of 15 V (the green line) under pulsed pumping (I). Reflection POM images of the N/BP patterned coexistence for testing the laser performance (II). The scale bar is 200  $\mu\text{m}$ .

would exhibit fruitful physical and optical phenomenon for both scientific and technologic innovations. The reflection band of BP regions was determined by the periodicity of the lattice and could be adjusted by modulating either the chiral dopant content of the prepolymerized mixture (Figure S8, Supporting Information) or the chirality of the LCs refilled into the polymer network (Figure S2, Supporting Information) to achieve a spectral match of the resonating wavelength with the gain spectrum under a pumping excitation (Figure S8, Supporting Information). The emission spectrum of such bi-phase coexistence exhibited a specific characteristic having a main sharp peak overlapping an amplified spontaneous emission (ASE) background caused by the coexistence of the regular photonic lattice of BP and the lattice-less nematic phase (Figure 4c). An interesting red-shift for less than 5 nm of the main peak, compared to the laser emission of pure BP, was found. Such a tiny but perceptible shift was probably due to a spectral broadening of the reflection band in BP/N bi-phase coexistence, rather than a coincidence. Normally, the ASE background of a laser is considered to be non-profitable and undesirable mainly due to the reduction of laser coherence. However, such a narrow-bandwidth laser emission with an ASE background may have

its own specific application in confidential fiber communication, wherein the background reduces the coherent length, and thus the original interference information is destroyed once someone intends to extract the information, while the recovery of the information at the receiving terminal can be achieved via a narrow-band detector to read the original information carried by the main peak. Moreover, the emission intensity can be readily modulated conveniently by applying an external stimulation of 15 V to induce a lattice deformation of BP regions, thus enabling a manipulation of the coherence which is still a formidable challenge in laser technology.

The fast development of technological applications places stringent requirements on the foundations of novel materials in terms of their physical, biological, optical, and chemical properties, which may be obtained in a coexistence system of materials or phases with distinct molecular arrangement and symmetry. In this work, a fantastic bi-phase LC patterned coexistence of the optically achiral-anisotropic N phase and the optically chiral-isotropic BPII with dynamic and reversible stimuli-responsive chirality and anisotropy was achieved using localized micro-regional polymer templating technique. The deliberately optimized material system could precisely

record the information of the LC director alignment arrangement utilizing the localized 3D polymer networks and could subsequently transfer the information to the achiral LC to restore the original 3D lattice architecture via the delicate equilibrium between achiral–chiral interaction and interfacial free energy between LCs and polymer. The patterned distribution of phases in such coexistence system can be readily tailored by a prescribed template. One specific feature of the patterned coexistence system which has not been demonstrated previously was the dynamic and reversible responsive chirality and anisotropy, having the capability of reversible transformation from the original optically achiral/chiral and anisotropic–isotropic state to the achiral/chiral but entirely optically isotropic state by the external stimulation of a weak electric field. Further enhancing the electric field to an unwound strength of the helix triggered the system to a uniform achiral and isotropic state. Practical applications of the soft patterned coexistence, such as the multi-mode passive display and the specific micro-cavity laser emission, are demonstrated using the bi-phase patterns. This multi-mode passive display combines the lattice effect of BP and birefringence effect of the N phase, which can be switched without the external field and applied to static display devices. The laser emission of the BP/N coexistence system with a narrow band-width peak and a broadened ASE background provides a low coherence, which might be promising to the confidential fiber communication. Moreover, it proposes an efficient approach to conveniently modulate the birefringence of the LCs confined in such a thin film by strategically “kneading” one optically anisotropic phase together with another optically isotropic one by varying the shape, size, or the density of the BP area through a prescribed patterned exposure. Such soft patterned coexistence system could profoundly facilitate the understanding of the formation, arrangement, and dynamics of soft condensed matter leading toward diverse technological applications.

## Experimental Section

**Material Preparation:** The initial chiral LC mixture for fabricating the patterned polymer template contains the commercially available eutectic nematic LC (TEB300, Slichem), a chiral dopant (R5011, HCH), reactive monomers (RM257, Merck; EHA, Adams), and the photoinitiator IRG184 (Energy Chemical). The mixture was stirred at a temperature of 70 °C (beyond the clearing point of the nematic LC host) for at least 1 h and was then injected into the 4- $\mu$ m-thick LC cell assembled from two indium tin oxide coated glass substrates with planar alignment. The sample was settled on a hot stage (LTS120E, Linkam) and cooled from the clearing point at a rate of 0.2 °C min<sup>-1</sup>. As the temperature decreased to 36 °C, a Bragg reflection around 540 nm appeared, indicating the presence of the BP. As the temperature further decreased, the reflection peak continuously blue-shifted to 510 nm. It is preferred to record and stabilize the LC director alignment in the BP11 to prove the success of localized micro-regional polymer templating technique, so the sample was exposed by a 365 nm UV collimating lamp (Lamplic UVCE-4) with 5 mW cm<sup>-2</sup> for 4 min through a photomask with periodic square patterns (size: 60  $\mu$ m, spacing: 120  $\mu$ m) at 34.5 °C. After UV curing, the sample was immersed in dichloromethane for 36 h to wash out the LC host, oligomers, and unpolymerized monomers. Then, the sample was placed on the hot stage at 60 °C for 1 h to remove the residue solvent, leaving behind the patterned polymer template. The nematic LC TEB300 was refilled into the cell at a temperature of 70 °C by

the capillary effect. The sample was then cooled to room temperature to obtain a stable achiral-anisotropic and chiral-isotropic coexistence.

**Optical Characterization:** A POM (Nikon LV100 POL, Avantes) equipped with a CCD (DS-U3, Nikon) and a spectrometer (ULS2048, Avantes) was used to capture the POM textures and to investigate the spectra of the sample under both transmission and reflection modes. The corresponding Kössel diagram was detected in the reflection mode with a monochromatic laser source (450 nm) and a high numerical aperture (NA) oil immersed objective ( $\times 100$ /NA = 1.25, oil, Plan, Nikon) and was received at the back focal plane of the objective. Sample birefringence was measured using the conventional Senarmont's compensation method, in which the horizontally polarized He-Ne laser (633 nm) passes normally in sequence the sample (the sample axis at 45° with the incident polarization), the 633 nm quarter wave plate (the crystal axis in parallel with the incident polarization), the analyzing polarizer (in perpendicular with the incident polarization), and the optical power-meter (Thorlabs, PM320E) and the sample birefringence was calculated from the transmitted intensity. The sample for testing the laser performance was prepared by refilling the nematic LC TEB300 doped with 0.5 wt% laser dye (4-(dicyanomethylene)-2-methyl-6-(4-dimethylaminostyryl)-4H-pyran) into the cell with the polymer template. For pumping, a pulsed frequency-doubled Nd:YAG laser (532 nm, 7 Hz) was focused by a spherical lens into the pumping spot (with a diameter of 200  $\mu$ m) onto the sample where the pump energy was adjusted by the adjustable attenuation plate. Laser emission to the sample normal was received by an optical fiber and analyzed using a high-resolution spectrometer (ULS2048, Avantes).

## Supporting Information

Supporting Information is available from the Wiley Online Library or from the author.

## Acknowledgements

Q.M., B.L., and W.H. contributed equally to this work. The authors acknowledge the support from the National Key Research and Development Program of China (2017YFA0303700), the National Science Foundation of China (grant nos. 61822504, 61575063, 61435008, and 51873060), the Shanghai Rising Star Program (grant no. 17QA1401100), and the State Key Laboratory of Applied Optics (no. M200-D-1716).

## Conflict of Interest

The authors declare no conflict of interest.

## Keywords

anisotropic phase, chirality, isotropic phase, soft matter, stimuli-responsive behavior

Received: January 27, 2020

Revised: May 26, 2020

Published online: June 22, 2020

- [1] T. Sekitani, U. Zschieschang, H. Klauk, T. Someya, *Nat. Mater.* **2010**, 9, 1015.
- [2] B. C.-K. Tee, C. Wang, R. Allen, Z. Bao, *Nat. Nanotechnol.* **2012**, 7, 825.



- [3] S. I. Rich, R. J. Wood, C. Majidi, *Nat. Electron.* **2018**, 1, 102.
- [4] C. M. Yakacki, R. Shandas, D. Safranski, A. M. Ortega, K. Sassaman, K. Gall, *Adv. Funct. Mater.* **2008**, 18, 2428.
- [5] a) S. Ramakrishna, J. Mayer, E. Wintermantel, K. W. Leong, *Compos. Sci. Technol.* **2001**, 61, 1189; b) Z. Zheng, C. Yuan, W. Hu, H. K. Bisoyi, M. Tang, Z. Liu, P. Sun, W. Yang, X. Wang, D. Shen, Y. Li, F. Ye, Y. Lu, G. Li, Q. Li, *Adv. Mater.* **2017**, 29, 1703165.
- [6] T. Takeichi, Y. Saito, T. Agag, H. Muto, T. Kawauchi, *Polymer* **2008**, 49, 1173.
- [7] K. Noda, T. Yasuda, Y. Nishi, *Electrochim. Acta* **2004**, 50, 243.
- [8] B. J. Schmitt, *Angew. Chem. Int. Ed.* **1979**, 18, 273.
- [9] H.-A. Klok, S. Lecommandoux, *Adv. Mater.* **2001**, 13, 1217.
- [10] W. A. Lopes, H. M. Jaeger, *Nature* **2001**, 414, 735.
- [11] D. R. Paul, J. W. Barlow, *J. Macromol. Sci., Rev. Macromol. Chem.* **1980**, 18, 109.
- [12] S. Y. Heriot, R. A. L. Jones, *Nat. Mater.* **2005**, 4, 782.
- [13] a) H. Lu, Y. Liu, J. Gou, J. Leng, S. Du, *Appl. Phys. Lett.* **2010**, 96, 084102; b) J. S. Leng, W. M. Huang, X. Lan, Y. J. Liu, S. Y. Du, *Appl. Phys. Lett.* **2008**, 92, 204101; c) S. Yun, X. Niu, Z. Yu, W. Hu, P. Brochu, Q. Pei, *Adv. Mater.* **2012**, 24, 1321; d) J. S. Leng, X. Lan, Y. J. Liu, S. Y. Du, W. M. Huang, N. Liu, S. J. Phee, Q. Yuan, *Appl. Phys. Lett.* **2008**, 92, 014104.
- [14] a) M. Raja, S. H. Ryu, A. M. Shanmugharaj, *Eur. Polym. J.* **2013**, 49, 3492; b) W.-J. Zhang, *J. Power Sources* **2011**, 196, 13.
- [15] a) *Nanoscience with Liquid Crystals: From Self-Organized Nanostructures to Applications* (Ed: Q. Li), Springer, Heidelberg **2014**; b) *Liquid Crystals Beyond Displays: Chemistry, Physics, and Applications* (Ed: Q. Li), John Wiley & Sons, Hoboken, NJ **2012**.
- [16] a) Y. Wang, Q. Li, *Adv. Mater.* **2012**, 24, 1926; b) H. K. Bisoyi, Q. Li, *Acc. Chem. Res.* **2014**, 47, 3184; c) H. K. Bisoyi, Q. Li, *Angew. Chem. Int. Ed.* **2016**, 55, 2994; d) L. Wang, Q. Li, *Adv. Funct. Mater.* **2016**, 26, 10; e) R. S. Zola, H. Bisoyi, H. Wang, A. Urbas, T. J. Bunning, Q. Li, *Adv. Mater.* **2019**, 31, 1806172.
- [17] a) H. K. Bisoyi, Q. Li, *Chem. Rev.* **2016**, 116, 15089; b) L. Wang, H. K. Bisoyi, Z. Zheng, K. G. Gutierrez-Cuevas, G. Singh, S. Kumar, T. J. Bunning, Q. Li, *Mater. Today* **2017**, 20, 230; c) H. Bisoyi, Q. Li, *Prog. Mater. Sci.* **2019**, 104, 1.
- [18] a) L. Wang, A. Urbas, Q. Li, *Adv. Mater.* **2018**, 1801335; b) H. K. Bisoyi, T. J. Bunning, Q. Li, *Adv. Mater.* **2018**, 30, 1706512; c) T.-H. Lin, Y. Li, C.-T. Wang, H.-C. Jau, C.-W. Chen, C.-C. Li, H. K. Bisoyi, T. J. Bunning, Q. Li, *Adv. Mater.* **2013**, 25, 5050; d) Z. Zheng, Y. Li, H. K. Bisoyi, L. Wang, T. J. Bunning, Q. Li, *Nature* **2016**, 531, 352.
- [19] J. S. Lintuvuori, K. Stratford, M. E. Cates, D. Marenduzzo, *Phys. Rev. Lett.* **2018**, 121, 037802.
- [20] J. A. Martínez-González, Y. Zhou, M. Rahimi, E. Bukusoglu, N. L. Abbott, J. J. de Pablo, *Proc. Natl. Acad. Sci. USA* **2015**, 112, 13195.
- [21] E. Bukusoglu, X. Wang, J. A. Martínez-González, J. J. de Pablo, N. L. Abbott, *Adv. Mater.* **2015**, 27, 6892.
- [22] a) M. Humar, I. Mušević, *Opt. Express* **2010**, 18, 26995; b) L. Chen, Y. Li, J. Fan, H. K. Bisoyi, D. A. Weitz, Q. Li, *Adv. Opt. Mater.* **2014**, 2, 845; c) J. Fan, Y. Li, H. K. Bisoyi, R. S. Zola, D. Yang, T. J. Bunning, D. A. Weitz, Q. Li, *Angew. Chem. Int. Ed.* **2015**, 54, 2160.
- [23] H. Kikuchi, M. Yokota, Y. Hisakado, H. Yang, T. Kajiyama, *Nat. Mater.* **2002**, 1, 64.
- [24] L. Rao, Z. Ge, S.-T. Wu, S. H. Lee, *Appl. Phys. Lett.* **2009**, 95, 231101.
- [25] S. Yokoyama, S. Mashiko, H. Kikuchi, K. Uchida, T. Nagamura, *Adv. Mater.* **2006**, 18, 48.
- [26] M. Wang, C. Zou, J. Sun, L. Zhang, L. Wang, J. Xiao, F. Li, P. Song, H. Yang, *Adv. Funct. Mater.* **2017**, 27, 1702261.
- [27] K. J. Vahala, *Nature* **2003**, 424, 839.
- [28] F. Castles, F. V. Day, S. M. Morris, D. H. Ko, D. J. Gardiner, M. M. Qasim, S. Nosheen, P. J. Hands, S. S. Choi, R. H. Friend, H. J. Coles, *Nat. Mater.* **2012**, 11, 599.
- [29] Z. Zheng, J. Song, Y. Liu, F. Guo, J. Ma, L. Xuan, *Liq. Cryst.* **2008**, 35, 489.
- [30] L. He, Ş. K. Özdemir, L. Yang, *Laser Photon. Rev.* **2012**, 7, 60.
- [31] W. Huang, C.-I. Yuan, D. Shen, Z.-g. Zheng, *J. Mater. Chem. C* **2017**, 5, 6923.
- [32] R. F. Oulton, V. J. Sorger, T. Zentgraf, R.-M. Ma, C. Gladden, L. Dai, G. Bartal, X. Zhang, *Nature* **2009**, 461, 629.